Supplementary Material

Enhanced Photocatalytic Hydrogen Peroxide Production over g-C_3N_4/MoS_2 composites through Phase-Interface Engineering: Electron Transfer and Synergy Mechanism

Yuxing Cai, Keqiang Shi, Cheng-Chao Jin*, Rongrong Jia, Jian-Hao Wu, Xiaozhuo Wang, Mengshan Hou, Chenghao Bao, Lan Li, Zhi Chen*

College of Materials and Chemistry, China Jiliang University, Hangzhou 310018, P. R. China.

*Corresponding authors: ccjin_cn@163.com (C. Jin); zchen@cjlu.edu.cn (Z. Chen).

Figures

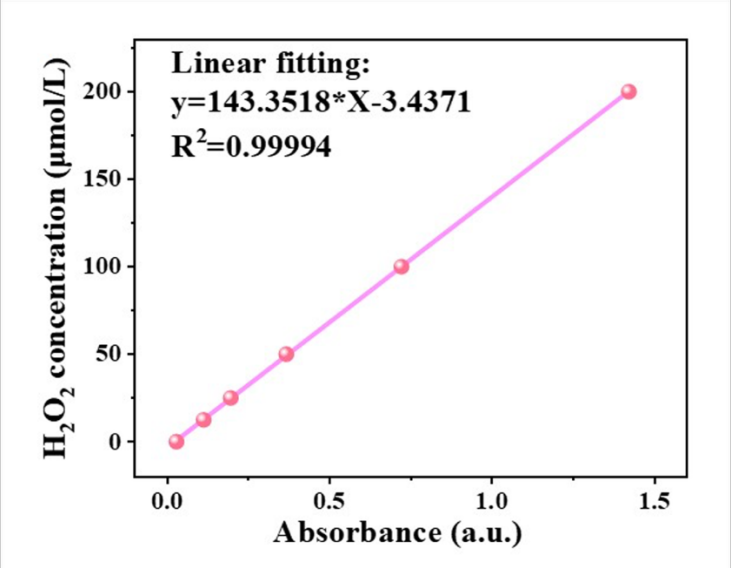

Fig. S1 Linear fitting equation of H_2O_2 concentration determined by iodimetry.

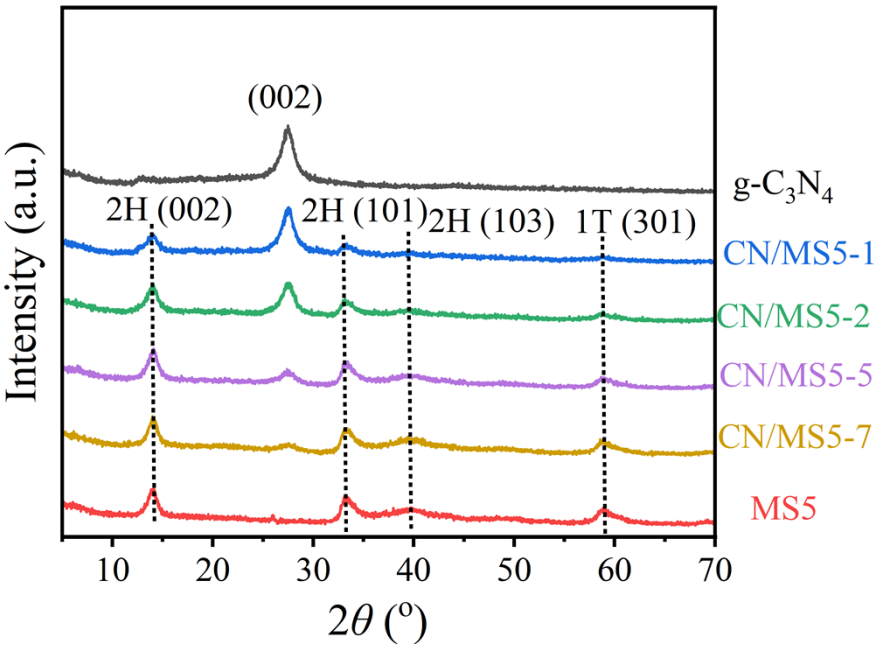

Fig. S2 XRD patterns of the CN/MS5-based heterojunctions

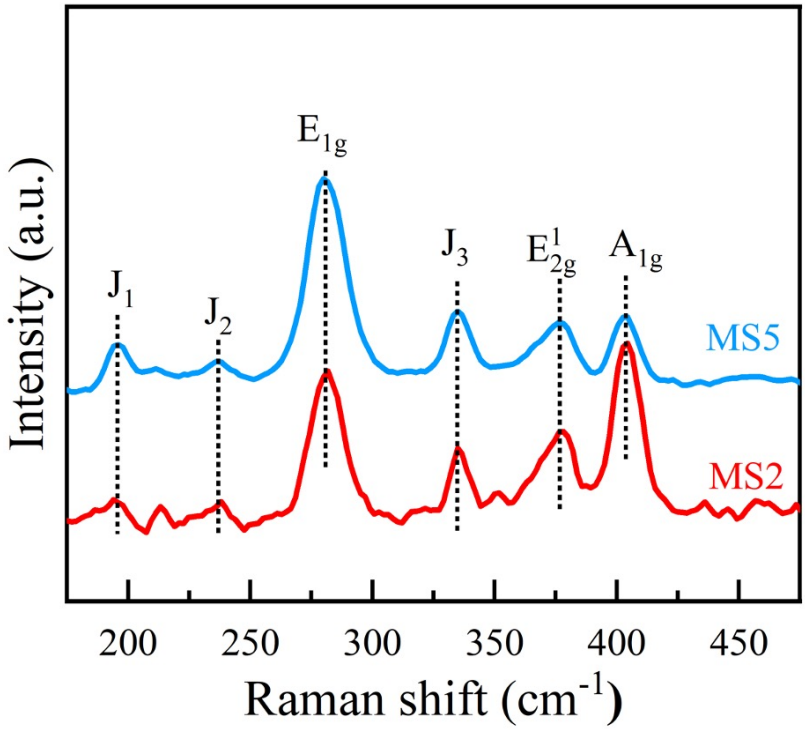

Fig. S3 Raman spectra of MS2 and MS5

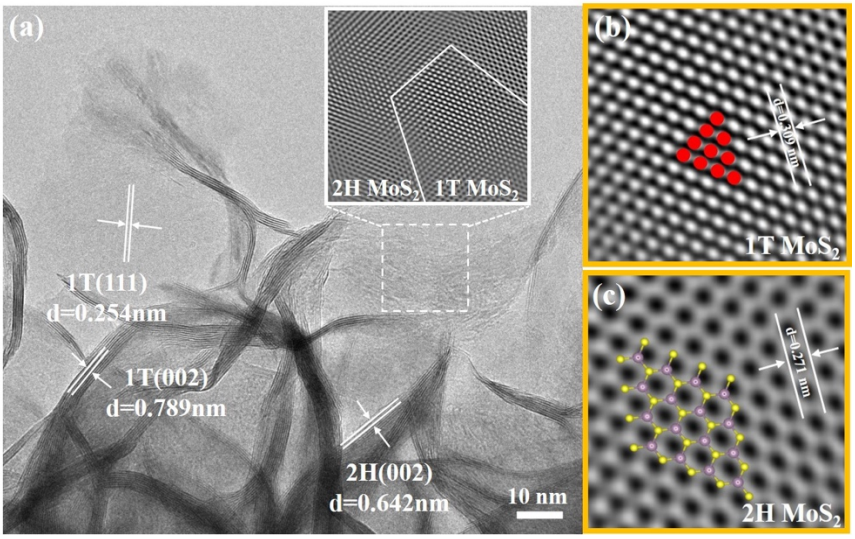

Fig. S4 (a) TEM image of MS2. HRTEM images for (b) 1T-phase MoS_2 and (c) 2H-phase MoS_2, respectively.

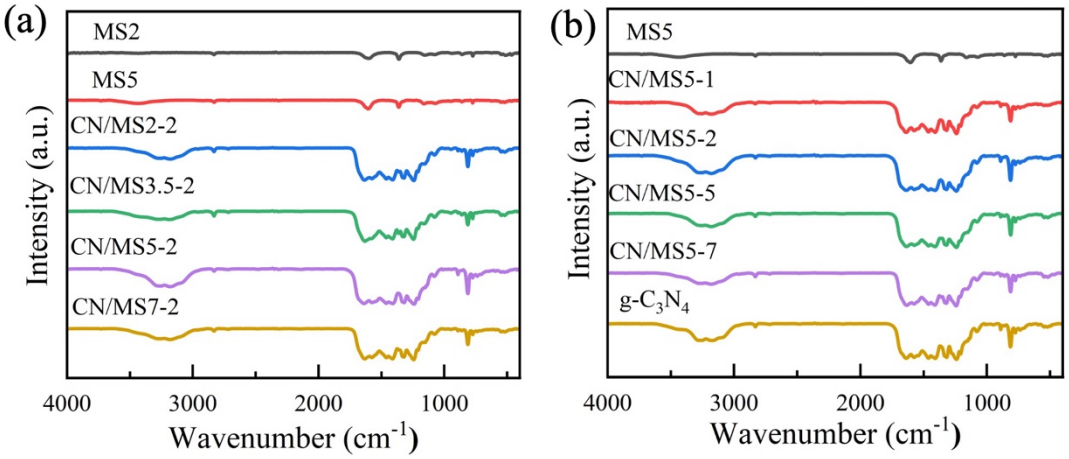

Fig. S5 FT-IR spectra of various samples.

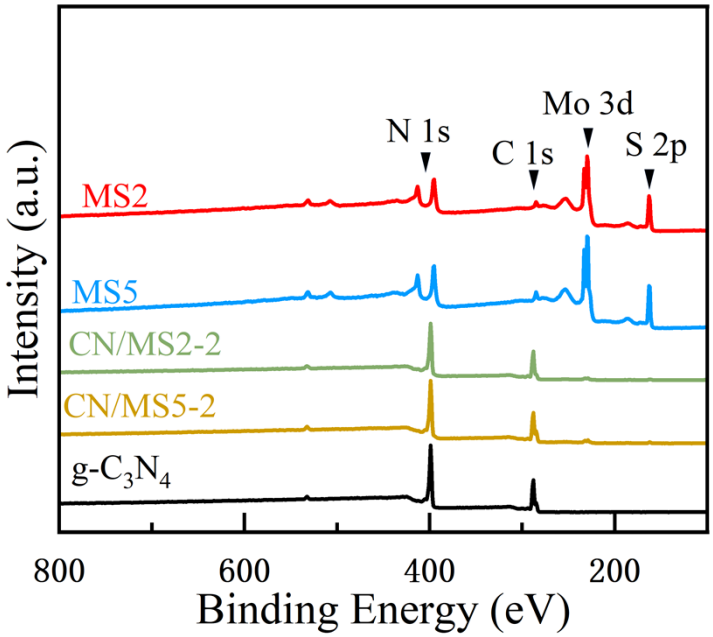

Fig. S6 XPS spectra of g-C_3N_4, MS2, MS5, CN/MS2-2, and CN/MS5-2.

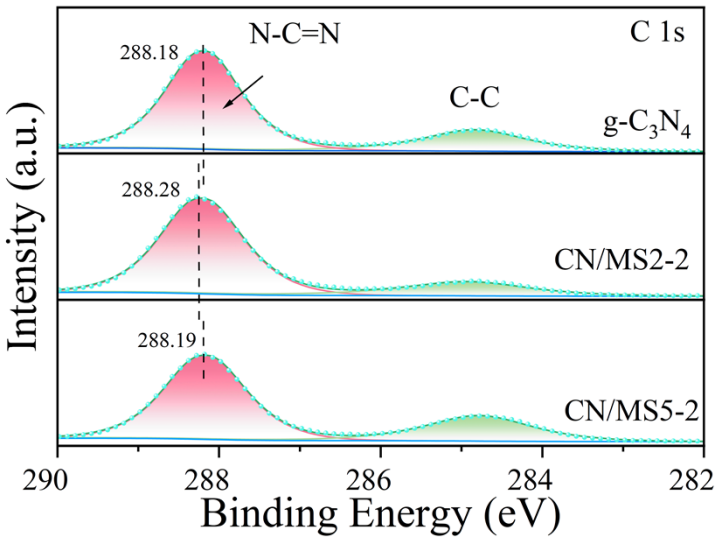

Fig. S7 High-resolution XPS spectra of C 1s

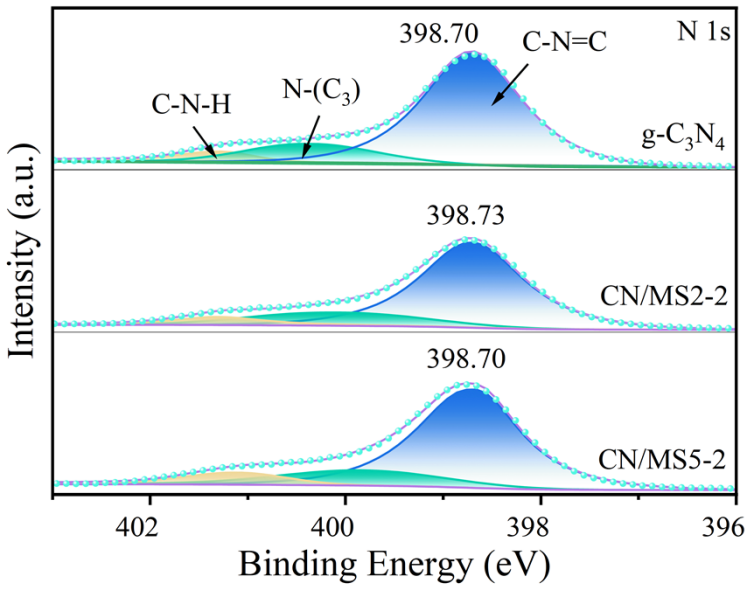

Fig. S8 High-resolution XPS spectra of N 1s

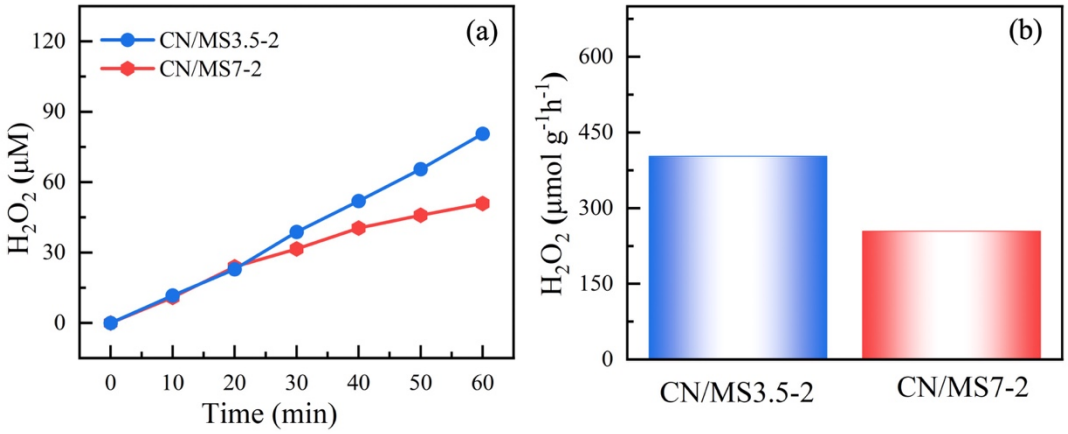

Fig. S9 Photocatalytic H_2O_2 production and corresponding yield on CN/MS3.5-2 and CN/MS7-2 catalysts.

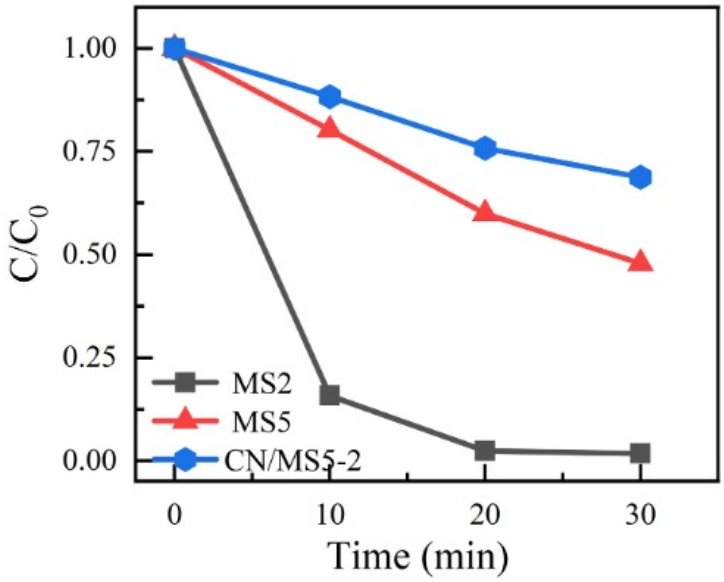

Fig. S10 Decomposition of H_2O_2 by MS2, MS5, and CN/MS5-2 under N_2 conditions

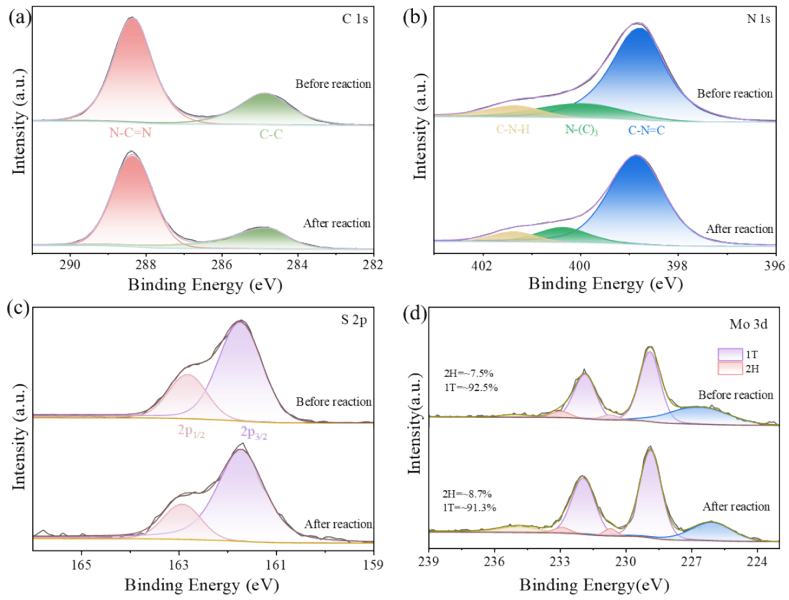

Fig. S11 High-resolution XPS spectra of (a) C 1s, (b) N 1s, (c) 2p, and (d) Mo 3d for CN/MS5-2 before and after photocatalytic reaction.

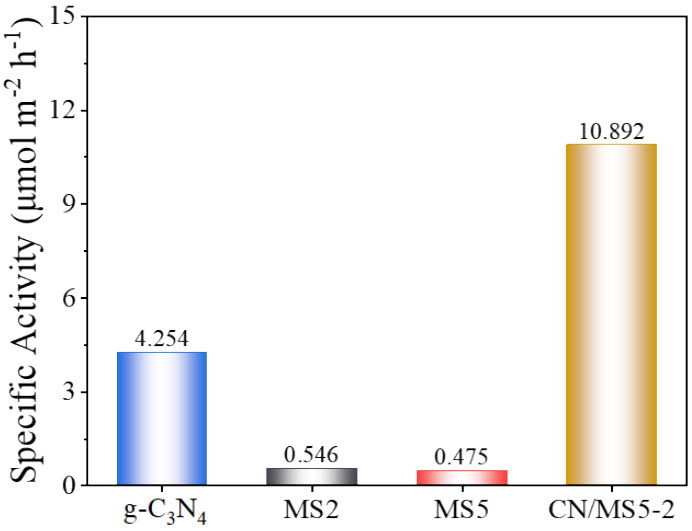

Fig. S12 Unit area activity of the sample

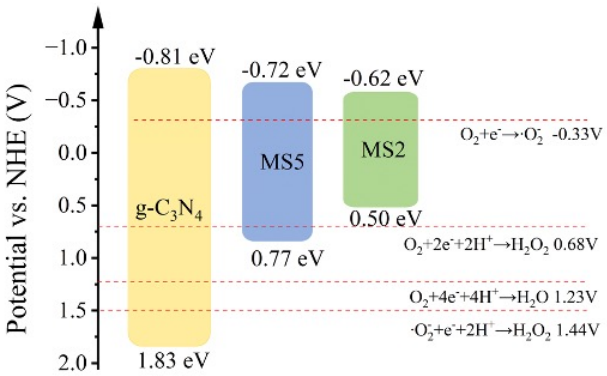

Fig. S13 Energy band structures for g-C_3N_4, MS2, and MS5.

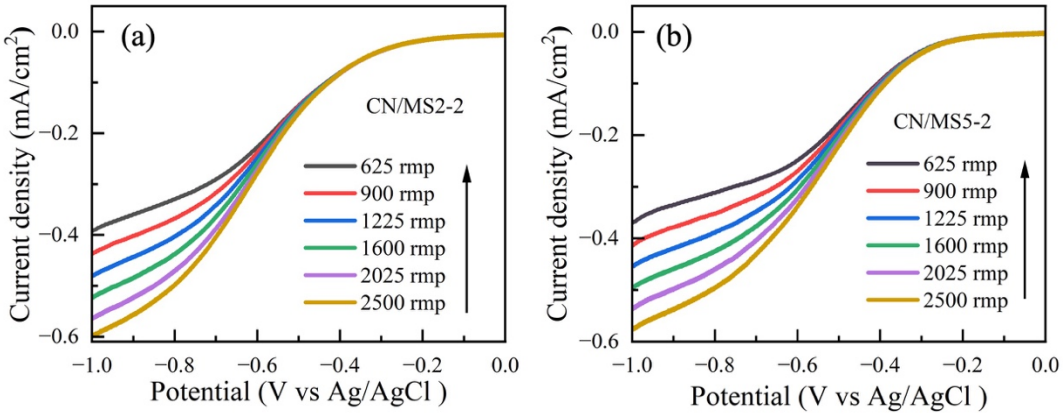

Fig. S14 LSV curves of (a) CN/MS2-2 and (b) CN/MS5-2.